JOURNAL OF MAGNETIC RESONANCE, Series B 103, 247–254 (1994)

Estimation of the Effective Self-Diffusion *Tensor* from the NMR Spin Echo

PETER J. BASSER,* JAMES MATTIELLO,* AND DENIS LEBIHAN†

* *Biomedical Engineering and Instrumentation Program, National Center for Research Resources, and* † *Diagnostic Radiology Department, The Warren G. Magnuson Clinical Center, National Institutes of Health, Bethesda, Maryland 20892*

Received July 28, 1992; revised May 24, 1993

The diagonal and off-diagonal elements of the effective self-diffusion tensor, $\mathbf{D}^{\text{eff}}$, are related to the echo intensity in an NMR spin-echo experiment. This relationship is used to design experiments from which $\mathbf{D}^{\text{eff}}$ is estimated. This estimate is validated using isotropic and anisotropic media, i.e., water and skeletal muscle. It is shown that significant errors are made in diffusion NMR spectroscopy and imaging of anisotropic skeletal muscle when off-diagonal elements of $\mathbf{D}^{\text{eff}}$ are ignored, most notably the loss of information needed to determine fiber orientation. Estimation of $\mathbf{D}^{\text{eff}}$ provides the theoretical basis for a new MRI modality, diffusion *tensor* imaging, which provides information about tissue microstructure and its physiologic state not contained in scalar quantities such as T_1, T_2, proton density, or the scalar apparent diffusion constant. © 1994 Academic Press, Inc.

INTRODUCTION

A scalar self-diffusivity, D, has been measured accurately in water and other isotropic media using NMR spin-echo (*1, 2*) and pulsed-gradient spin-echo (*3*) sequences. It is estimated from the linear relationship between the logarithm of the echo intensity and the magnitude of the magnetic-field gradient in which D appears as a constant of proportionality (*1, 3*). When diffusion NMR spectroscopy and Fourier NMR imaging were combined recently (*4–6*) by including diffusion gradients within an imaging sequence, an effective diffusivity, D^{eff}, could then be estimated in each voxel of an image (*7*).

In contrast to isotropic media, one observes significantly different effective diffusion constants in anisotropic media when diffusion gradients are applied in different directions. For instance, in diffusion NMR spectroscopy and imaging of anisotropic tissue like brain white matter (*8*) and skeletal muscle (*9*), the observed echo intensity depends on the specimen's orientation with respect to the direction of the applied magnetic-field gradient. The orientation dependence of diffusion can be characterized by $\mathbf{D}^{\text{eff}}$, an effective self-diffusion tensor (*10–14*). While its use has been suggested in NMR spectroscopy (*3*) and imaging (*7, 15*), to our knowledge an explicit relationship between the effective self-diffusion tensor and the NMR signal has not been elucidated. Moreover, the off-diagonal elements of $\mathbf{D}^{\text{eff}}$ have not been measured or even considered. Their importance cannot be minimized (*16*). Although differences among $\mathbf{D}^{\text{eff}}$'s diagonal elements, D^{eff}_{xx}, D^{eff}_{yy}, and D^{eff}_{zz}, are a necessary condition to demonstrate anisotropic diffusion, all diagonal and off-diagonal elements of $\mathbf{D}^{\text{eff}}$ must be known to characterize it adequately, and specifically to infer the mean microscopic displacements of protons.[1]

In this paper, we show how to calculate the effects of anisotropic diffusion on the NMR signal in imaging and spectroscopy by relating the diagonal and off-diagonal elements of $\mathbf{D}^{\text{eff}}$ to the measured echo intensity in a pulsed-gradient, spin-echo experiment. We then design a series of magnetic-field-gradient sequences that permit us to observe the effects of different linear combinations of these diagonal and off-diagonal elements of $\mathbf{D}^{\text{eff}}$ on the measured echo. Next, treating the components of $\mathbf{D}^{\text{eff}}$ as free parameters, we show how to estimate them in a voxel from the measured spin-echo intensity and how to assess their importance, especially that of the off-diagonal elements. This work leads to methods that can be used to determine fiber orientation *in vivo* (*17*), to infer the microscopic displacements of protons and other moieties *in vivo*, and to correct for cross talk, misalignment, and maladjustment of magnetic-gradient coils.

THEORY

The Macroscopic Effective Self-Diffusion Tensor, $\mathbf{D}^{\text{eff}}$

The effective second-order self-diffusion tensor, $\mathbf{D}^{\text{eff}}$, relates the macroscopic concentration gradient, ∇C, and macroscopic diffusive flux, $\mathbf{J}$, in an anisotropic medium:

[1] Alternatively, it is sufficient to know the eigenvalues and eigenvectors of $\mathbf{D}^{\text{eff}}$.

1064-1866/94 $6.00
Copyright © 1994 by Academic Press, Inc.
All rights of reproduction in any form reserved.

$\mathbf{J} = -\mathbf{D}^{\text{eff}}\nabla C$ or

$$\begin{bmatrix} J_x \\ J_y \\ J_z \end{bmatrix} = -\begin{bmatrix} D_{xx}^{\text{eff}} & D_{xy}^{\text{eff}} & D_{xz}^{\text{eff}} \\ D_{yx}^{\text{eff}} & D_{yy}^{\text{eff}} & D_{yz}^{\text{eff}} \\ D_{zx}^{\text{eff}} & D_{zy}^{\text{eff}} & D_{zz}^{\text{eff}} \end{bmatrix} \begin{bmatrix} \dfrac{\partial C}{\partial x} \\ \dfrac{\partial C}{\partial y} \\ \dfrac{\partial C}{\partial z} \end{bmatrix}. \quad [1]$$

Diagonal elements of $\mathbf{D}^{\text{eff}}$ scale fluxes and concentration gradients in the same direction; off-diagonal elements couple fluxes and concentration gradients in orthogonal directions. One important consequence of Eq. [1] is that the concentration gradient (vector) is not necessarily parallel to the diffusive flux (vector), as in isotropic media. For uncharged moieties such as water, $\mathbf{D}^{\text{eff}}$ is symmetric (*10–14*) (i.e., $\mathbf{D}^{\text{eff}} = \mathbf{D}^{\text{eff}\,\text{T}}$), a consequence of the reciprocity theorem and the principle of microscopic reversibility of nonequilibrium thermodynamics (*12, 13*).

One operational assumption made throughout this paper is that the components of the effective self-diffusion tensor are macroscopic, voxel-averaged quantities that are not explicit functions of time and may vary among voxels.

Relating Echo Intensity and $\mathbf{D}^{\text{eff}}$ in a Spin-Echo, Pulsed-Gradient NMR Experiment

The solution to the Bloch equations (*18*) with diffusion (*19*) in a 90°–180° spin-echo, pulsed-gradient experiment is well known, as is the modification of Stejskal that makes them amenable to describing free diffusion in an anisotropic medium (*14*). Stejskal (*14*) related the applied magnetic-field-gradient vector, $\mathbf{G}(t)$,

$$\mathbf{G}(t) = [G_x(t), G_y(t), G_z(t)]^{\text{T}}, \quad [2a]$$

and its time integral,

$$\mathbf{F}(t) = \int_0^t \mathbf{G}(t')dt', \quad [2b]$$

to the echo intensity, $A(\text{TE})$, in a spin-echo experiment according to[2]

$$\frac{A(\text{TE})}{A(0)} = \exp\left(-\gamma^2 \int_0^{\text{TE}} \left[\mathbf{F}(t') - 2H\left(t' - \frac{\text{TE}}{2}\right)\mathbf{f}\right]^{\text{T}} \mathbf{D} \times \left[\mathbf{F}(t') - 2H\left(t' - \frac{\text{TE}}{2}\right)\mathbf{f}\right] dt'\right), \quad [3]$$

[2] We have rewritten the integrand of Eq. [3] in matrix notation to emphasize that it is a quadratic form.

where γ is the gyromagnetic ratio of protons, $A(0)$ is the echo intensity with no applied gradients, $H(t')$ is the unit Heaviside function, TE is the echo time, and $\mathbf{f} = \mathbf{F}(\text{TE}/2)$.

By analogy with the definition of the scalar effective diffusion coefficient (*20*), we define the effective diffusivity tensor, $\mathbf{D}^{\text{eff}}$, as a mean value of the exponent in Eq. [3] over the time interval [0, TE],

$$\gamma^2 \int_0^{\text{TE}} \left[\mathbf{F}(t') - 2H\left(t' - \frac{\text{TE}}{2}\right)\mathbf{f}\right] \times \left[\mathbf{F}(t') - 2H\left(t' - \frac{\text{TE}}{2}\right)\mathbf{f}\right]^{\text{T}} dt' : \mathbf{D}^{\text{eff}} = \gamma^2 \int_0^{\text{TE}} \left[\mathbf{F}(t') - 2H\left(t' - \frac{\text{TE}}{2}\right)\mathbf{f}\right]^{\text{T}} \mathbf{D} \left[\mathbf{F}(t') - 2H\left(t' - \frac{\text{TE}}{2}\right)\mathbf{f}\right] dt', \quad [4]$$

where ":" is the generalized dot product. Taking the logarithm of Eq. [3] and using the definition of $\mathbf{D}^{\text{eff}}$, Eq. [4], we obtain

$$\ln\left[\frac{A(\text{TE})}{A(0)}\right] = -\sum_{i=1}^{3}\sum_{j=1}^{3} b_{ij}D_{ij}^{\text{eff}} = -\mathbf{b} : \mathbf{D}^{\text{eff}}. \quad [5]$$

The importance of Eq. [5] is that it establishes a *linear* relationship between the logarithm of the echo attenuation, $\ln[A(\text{TE})/A(0)]$, and each component of $\mathbf{D}^{\text{eff}}$, D_{ij}^{eff}. Above, b_{ij} is the ijth component of a symmetric matrix, $\mathbf{b}$, defined as

$$\mathbf{b} = \gamma^2 \int_0^{\text{TE}} \left[\mathbf{F}(t') - 2H\left(t' - \frac{\text{TE}}{2}\right)\mathbf{f}\right] \times \left[\mathbf{F}(t') - 2H\left(t' - \frac{\text{TE}}{2}\right)\mathbf{f}\right]^{\text{T}} dt'. \quad [6]$$

The b matrix above performs the role in anisotropic diffusion that the scalar b factor (i.e., the coefficient of the scalar effective diffusion constant) (*7*) performs in isotropic diffusion. While the diagonal elements, D_{xx}^{eff}, D_{yy}^{eff}, and D_{zz}^{eff}, and their respective coefficients, b_{xx}, b_{yy}, and b_{zz}, have been considered in the context of anisotropic diffusion spectroscopy and imaging (*15*), the remaining six off-diagonal elements of $\mathbf{D}^{\text{eff}}$, D_{xy}^{eff}, D_{xz}^{eff}, D_{yz}^{eff}, D_{yx}^{eff}, D_{zx}^{eff}, and D_{zy}^{eff}, and their respective coefficients, b_{xy}, b_{xz}, b_{yz}, b_{yx}, b_{zx}, and b_{zy}, have not. Note that the diagonal elements of b_{ij} subsume all interactions between diffusion and imaging gradient pulses in the same direction, which are referred to as "cross terms" (*6, 21*). However, the off-diagonal elements of b_{ij} couple imaging and diffusion gradients in *orthogonal* directions, which to date have been ignored.

Equation [5] above suggests that we can design experiments to observe different linear combinations of the com-

ponents of $\mathbf{D}^{\text{eff}}$ by applying diffusion gradients along various oblique directions. For example, to observe the echo attenuation caused only by D_{xx}^{eff}, we choose a gradient-pulse sequence in which $\mathbf{G}$ has a component only in the x direction, so that only $b_{11} = b_{xx} \neq 0$. Then,

$$\ln\left[\frac{A(\mathbf{b})}{A(0)}\right] = -b_{xx}D_{xx}^{\text{eff}}. \quad [7]$$

Alternatively, to observe the echo attenuation caused by all of the diagonal and off-diagonal components of $\mathbf{D}^{\text{eff}}$ simultaneously, we can choose all of the components of $\mathbf{G}$ to be nonzero, so that

$$\ln\left[\frac{A(\mathbf{b})}{A(0)}\right] = -[b_{xx}D_{xx}^{\text{eff}} + b_{yy}D_{yy}^{\text{eff}} + b_{zz}D_{zz}^{\text{eff}} + (b_{xy} + b_{yx})D_{xy}^{\text{eff}} + (b_{xz} + b_{zx})D_{xz}^{\text{eff}} + (b_{yz} + b_{zy})D_{yz}^{\text{eff}}]. \quad [8]$$

Moreover, for gradient-pulse sequences commonly used in diffusion spectroscopy (e.g., rectangular, sinusoidal, triangular, and trapezoidal), simple analytic expressions can be derived for each matrix element, b_{ij}. For example, for symmetric trapezoidal pulses like those shown in Fig. 1,

$$b_{ij} = \gamma^2 G_i G_j\left[\delta^2\left(\Delta - \frac{\delta}{3}\right) + \frac{\epsilon^3}{30} - \frac{\delta\epsilon^2}{6}\right], \quad [9]$$

where δ is the time between the initial rise of a trapezoidal pulse and the end of its plateau, Δ is the time between the initial rise of the first and second pulses, ϵ is the rise time of the ramp, and G_i is the maximum field gradient along the x_i coordinate direction. By substituting Eq. [9] into Eq. [5], we derive a theoretical relationship between the echo attenuation, $A(\mathbf{b})$ [which is now written as $A(\mathbf{G})$] and $\mathbf{D}^{\text{eff}}$:

$$\ln\left[\frac{A(\mathbf{G})}{A(0)}\right] = -\gamma^2\left[\delta^2\left(\Delta - \frac{\delta}{3}\right) + \frac{\epsilon^3}{30} - \frac{\delta\epsilon^2}{6}\right]\mathbf{G}^T\mathbf{D}^{\text{eff}}\mathbf{G}. \quad [10]$$

The quadratic form in Eq. [10] reduces to a familiar expression when the medium is isotropic with diffusivity D_0,

$$\ln\left[\frac{A(\mathbf{G})}{A(0)}\right] = -\gamma^2|\mathbf{G}|^2\left[\delta^2\left(\Delta - \frac{\delta}{3}\right) + \frac{\epsilon^3}{30} - \frac{\delta\epsilon^2}{6}\right]D_0 = -bD_0, \quad [11]$$

a degenerate case of Eq. [10] for which the scalar b factor has already been derived (*22, 23*).

If there were no error in measuring the echo intensity, we could, in principle, determine the six independent elements of the effective self-diffusion tensor and $A(0)$ using only seven independent trials (i.e., in which $\mathbf{G}$ were chosen to lie in seven noncollinear directions) by simply inverting a 7×7

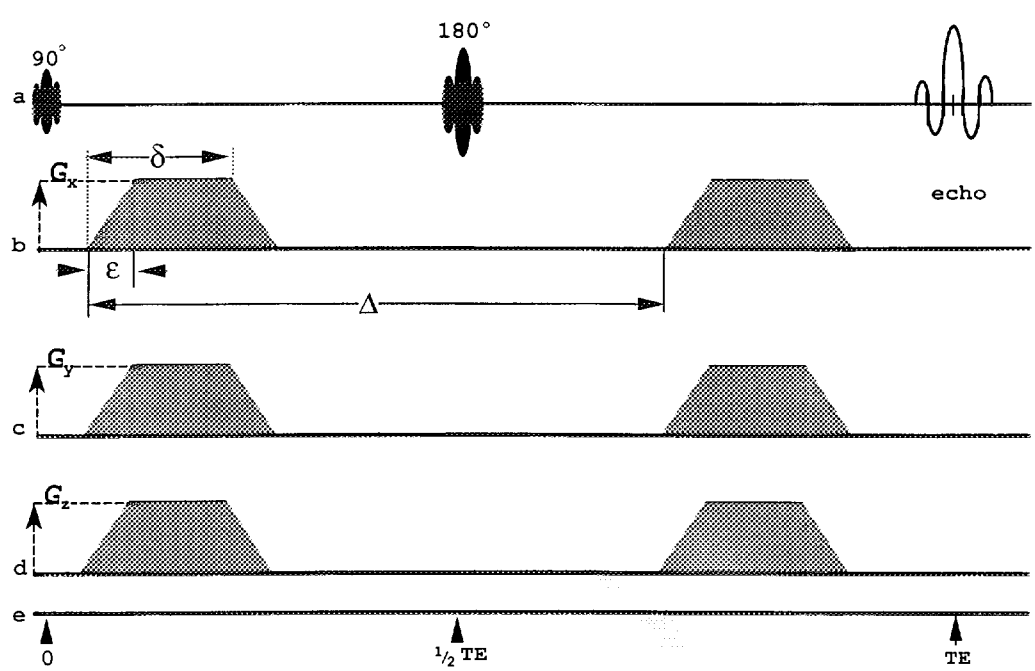

FIG. 1. Waveforms in a pulsed-gradient spin-echo diffusion spectroscopy experiment: (*a*) the 90° and 180° RF stimulating pulses from the surface coil; the magnetic field gradients (g/cm) applied in the (b) x, (c) y, and (d) z directions; (e) the time (TR = 15 s, TE = 40 ms, δ = 4.2 ms, ϵ = 0.2 ms, Δ = 22.5 ms). Gradients applied in different directions must be applied simultaneously.

matrix constructed from Eq. [10]. Since measurements of echo intensity are noisy, this approach provides poor estimates of $\mathbf{D}^{\text{eff}}$. Instead, we perform a much larger number of trials than seven to estimate $\mathbf{D}^{\text{eff}}$ statistically, and we use multivariate linear regression. In doing so, we do not neglect off-diagonal components of $\mathbf{D}^{\text{eff}}$ a priori, that is, we do not constrain them to be zero, as others have. Instead, we allow all components of $\mathbf{D}^{\text{eff}}$ to contribute to the measured echo intensity (as in Eq. [10]). Then, once all components of $\mathbf{D}^{\text{eff}}$ have been estimated, we can assess their relative importance.

MATERIALS AND METHODS

Estimation of $\mathbf{D}^{\text{eff}}$ from Spin-Echo Intensity Measurements

We use multivariate linear regression (*24*) of Eq. [10] to estimate the components of $\mathbf{D}^{\text{eff}}$ in a voxel. Echo intensities are measured for a series of symmetric, trapezoidal gradient-pulse sequences in which magnetic-field gradients are applied in at least seven noncollinear directions. The optimal $\mathbf{D}^{\text{eff}}$ minimizes the sum of the squares of the difference between the measured and the theoretically predicted spin-echo intensities.

In general, in each experiment, we choose n noncollinear gradient directions, for which m measurements of $A(\mathbf{G})$ are made at different gradient strengths. These $n \times m$ observations of $\ln[A(\mathbf{G})]$ are stored as an $nm \times 1$ column vector, $\mathbf{x}$. We define another column vector of parameters to be estimated, α, which has seven elements—the six independent elements of $\mathbf{D}^{\text{eff}}$ and $\ln[A(0)]$:

$$\alpha = \{D^{\text{eff}}_{xx}, D^{\text{eff}}_{yy}, D^{\text{eff}}_{zz}, D^{\text{eff}}_{xy}, D^{\text{eff}}_{xz}, D^{\text{eff}}_{yz}, \ln[A(0)]\}^{\mathrm{T}}. \quad [12]$$

Next, we define an $nm \times 1$ column vector of predicted outcomes, ξ, as the product of an $nm \times 7$ matrix of b matrix elements, $\mathbf{B}$, computed from Eq. [10], and α:

$$\xi = \mathbf{B}\alpha. \quad [13]$$

The χ^2 parameter, defined as

$$\chi^2(\xi) = (\mathbf{x} - \xi)^{\mathrm{T}}\mathbf{\Sigma}^{-1}(\mathbf{x} - \xi), \quad [14]$$

is the weighted sum of squares of deviations between the observed and the predicted echo intensities. For each of the $m \times n$ independent trials, the squared deviation is weighted by the corrected reciprocal error variance for that measurement, x_i^2/σ_{ii}^2, which become the diagonal elements of the covariance matrix, $\mathbf{\Sigma}^{-1}$. They account for the expected variation in each trial and correct for the distortion introduced by the logarithmic transformation of $A(\mathbf{G})/A(0)$ (*25*).

Minimizing $\chi^2(\xi)$ with respect to each of the seven unknown parameters in ξ yields seven linear (normal) equations, which in matrix form are

$$(\mathbf{B}^{\mathrm{T}}\mathbf{\Sigma}^{-1}\mathbf{B})\alpha_{\text{opt}} = (\mathbf{B}^{\mathrm{T}}\mathbf{\Sigma}^{-1})\mathbf{x}. \quad [15]$$

The optimal parameters, α_{opt}, are

$$\alpha_{\text{opt}} = (\mathbf{B}^{\mathrm{T}}\mathbf{\Sigma}^{-1}\mathbf{B})^{-1}(\mathbf{B}^{\mathrm{T}}\mathbf{\Sigma}^{-1})\mathbf{x} = \mathbf{M}^{-1}(\mathbf{B}^{\mathrm{T}}\mathbf{\Sigma}^{-1})\mathbf{x}. \quad [16]$$

The first term on the right-hand side of Eq. [16], $(\mathbf{B}^{\mathrm{T}}\mathbf{\Sigma}^{-1}\mathbf{B})^{-1} = \mathbf{M}^{-1}$, is a 7×7 matrix, the diagonal elements of which are the error variances of the seven estimated parameters.

Thus, in this section, we have reduced the problem of determining the components of the effective self-diffusion tensor to a routine problem in multivariate linear regression: solving seven linear (normal) equations simultaneously for seven unknown parameters.

EXPERIMENTAL

Diffusion spectroscopy and imaging of water and pork loin samples were performed on a 4.7 T spectrometer/imager (GE Omega, Fremont, California). The samples were placed on a surface coil and allowed to thermally equilibrate at 14.7°C in the bore of the magnet. The same surface coil can be used for both spectroscopy and imaging. A spin-echo, trapezoidal pulse-gradient sequence was used for diffusion spectroscopy with the isotropic and anisotropic samples and is shown in Fig. 1.

For water at 14.7°C, seven noncollinear magnetic-field-gradient directions were selected: $(G_x, G_y, G_z) = G_0\{(1, 0, 0), (0, 1, 0), (0, 0, 1), (1, 0, 1), (1, 1, 0), (0, 1, 1)$, and $(1, 1, 1)\}$. For each gradient direction, three trials were performed. In each trial, the gradient strength, G_0, was increased from 1 to 15 G/cm in increments of 1 G/cm. In all, 315 acquisitions were obtained for each sample.

This experimental protocol was repeated with an anisotropic pork-loin sample at 14.7°C. In one experiment, the muscle fibers of the pork-loin sample were approximately aligned with the x axis of the magnet; in another, the same sample was rotated about 40° in the plane of the xz axis.

RESULTS

Estimation of $\mathbf{D}^{\text{eff}}$ in an Isotropic Medium—Water

For water, the estimated effective self-diffusion tensor, $\mathbf{D}^{\text{est}}$, is given below with its standard error matrix:

$$\mathbf{D}^{\text{est}} = \left[\begin{pmatrix} 1.7003 & -0.0406 & 0.0027 \\ -0.0406 & 1.6388 & -0.0036 \\ 0.0027 & -0.0036 & 1.7007 \end{pmatrix} + \begin{pmatrix} \pm0.0057 & \pm0.0054 & \pm0.0055 \\ \pm0.0054 & \pm0.0056 & \pm0.0054 \\ \pm0.0055 & \pm0.0054 & \pm0.0057 \end{pmatrix}\right] \times 10^{-3}\,\frac{\text{mm}^2}{\text{s}}. \quad [17]$$

We use multiple hypothesis testing (*24*) to assess whether $\mathbf{D}^{est}$ is an isotropic matrix subject to explainable experimental statistical variability, with our null hypothesis being that the diffusion tensor is isotropic, i.e.,

$$\mathbf{D}^{null} = D_0\,\mathbf{I}, \quad \text{where } \mathbf{I} = \begin{bmatrix} 1 & 0 & 0 \\ 0 & 1 & 0 \\ 0 & 0 & 1 \end{bmatrix}. \qquad [18]$$

We estimate $\mathbf{D}^{eff}$ again from the same data set, now assuming the null hypothesis to be true. This reduced model (*24*) contains five linear constraint equations, three setting the off-diagonal elements to zero and two forcing the three diagonal elements to equal one another. Assuming the null hypothesis to be true, the estimated effective diffusion tensor is

$$\mathbf{D}^{est}_{null} = (1.6675 \pm 0.0033) \times 10^{-3}\,\frac{\text{mm}^2}{\text{s}}\,\mathbf{I}$$

or

$$D_0 = (1.6675 \pm 0.0033) \times 10^{-3}\,\frac{\text{mm}^2}{\text{s}}. \qquad [19]$$

The adjusted coefficient of determination $\rho^2 = 0.999999$ for $N = 315$.

To determine whether to accept or reject the null hypothesis, we use an F distribution. The relevant F statistic is (*26*)

$$F_0 = \frac{(R_c - R_u)/(k - r)}{R_c/[N - (k + 1)]}, \qquad [20]$$

where k and r are the number of free parameters in the unconstrained and constrained models, respectively; N is the total number of experimental data points; and R_u and R_c are the residual sums of squares for the unconstrained and constrained models, respectively.

For the water phantom, $r = 1$, $k = 7$, and $N = 315$, so that $F_0 = 21.5$ using Eq. [20]. But $F[k - r, N - (k + 1)] = 2.87$ and 2.13 for the 1 and 5% confidence limits, respectively; we would therefore reject the null hypothesis of isotropy. Indeed, these results may be explained by systematic instrumental errors discussed below.

Estimation of $\mathbf{D}^{eff}$ *in an Anisotropic Medium—Pork Skeletal Muscle*

The estimated diffusion tensor for the anisotropic pork sample with the fiber directions approximately aligned with the x axis is

$$\mathbf{D}^{est} = \left[\begin{pmatrix} 1.0513 & 0.0535 & -0.0040 \\ 0.0535 & 0.9697 & 0.0256 \\ -0.0040 & 0.0256 & 0.8423 \end{pmatrix} + \begin{pmatrix} \pm0.0055 & \pm0.0044 & \pm0.0043 \\ \pm0.0044 & \pm0.0053 & \pm0.0043 \\ \pm0.0043 & \pm0.0043 & \pm0.0051 \end{pmatrix}\right] \times 10^{-3}\,\frac{\text{mm}^2}{\text{s}} \qquad [21]$$

(adjusted $\rho^2 = 0.999999$; $N = 294$).

To represent the case in which the off-diagonal elements are ignored, we repeat the estimation of $\mathbf{D}^{eff}$ assuming the null hypothesis that the matrix is diagonal. We use three constraint equations to force all off-diagonal elements to be zero. Under these conditions, $r = 4$, $k = 7$, and $N = 294$, so that $F_0 = 38.49$ using Eq. [20]. Now $F[k - r, N - (k + 1)] = 3.85$ and 2.64 for the 1 and 5% confidence limits, respectively. We must therefore reject the null hypothesis that the matrix is diagonal.

In the second experiment with the same pork-loin sample, the fiber directions were rotated by approximately 40° with respect to the x axis in the x–z plane. The estimated diffusion tensor is now given by

$$\mathbf{D}^{est} = \left[\begin{pmatrix} 0.9761 & 0.0278 & -0.0748 \\ 0.0278 & 0.9529 & -0.0106 \\ -0.0748 & -0.0106 & 0.9653 \end{pmatrix} + \begin{pmatrix} \pm0.0039 & \pm0.0031 & \pm0.0031 \\ \pm0.0031 & \pm0.0039 & \pm0.0031 \\ \pm0.0031 & \pm0.0031 & \pm0.0039 \end{pmatrix}\right] \times 10^{-3}\,\frac{\text{mm}^2}{\text{s}} \qquad [22]$$

(adjusted $\rho^2 = 0.999999$; $N = 294$).

To represent the case in which the off-diagonal elements are ignored, we estimate $\mathbf{D}^{eff}$ assuming the null hypothesis that the matrix is diagonal. Under these conditions, $r = 4$, $k = 7$, and $N = 294$, so that $F_0 = 66.24$ using Eq. [20]. Again, $F[k - r, N - (k + 1)] = 3.85$ and 2.64 for the 1 and 5% confidence limits, respectively. We must therefore reject the null hypothesis that the estimated diffusion matrix for the rotated sample is diagonal.

In all of these experiments, our estimation of the error variance matrix, $\mathbf{\Sigma}^{-1}$, was corrected for the logarithmic transformation of the measured echo intensities, so that both the estimation of each component of the diffusion tensor and its error variance (given in $\mathbf{M}^{-1}$) were optimal. Independent trials were performed to estimate the error variance of $A(\mathbf{G})$, σ_{ii}^2, as a function of $|\mathbf{G}|$. They showed that $\sigma_{ii} \sim 150$ and were approximately uniform, independent of magnetic-field-gradient strength and direction. The estimated parameters obtained using weighted multivariate linear regression agreed with those obtained using a nonlinear Levenberg–Marquardt algorithm, using the untransformed form of Eq. [5] relating the echo intensity and the diffusion tensor:

$$A(\mathbf{b}) = A(0)\exp\left(-\sum_{i=1}^{3}\sum_{j=1}^{3} b_{ij}D_{ij}^{eff}\right). \qquad [23]$$

DISCUSSION

For both isotropic and anisotropic samples, standard errors were small compared with the estimated parameters, and the adjusted multiple coefficient of determination $\rho^2 \approx 1$ to

within six significant digits. This shows that the multivariate linear model (Eq. [5]) fits the data faithfully. In addition, the diffusivity, D_0 (in Eq. [19]), estimated by assuming water to be isotropic and homogeneous, is close to published values for water at 14.7°C (*7*). Despite this agreement, from our experimental data, the hypothesis that the estimated self-diffusion tensor for water is isotropic and homogeneous to within known instrumental variability should be rejected. The diagonal element D_{yy} differed from the other two by statistically significant amounts, and D_{xy} was significantly larger than zero. As self-diffusion of water is thought to be isotropic, this measured anisotropy must be the result of a systematic instrumental error, most likely a coupling between the x and y magnetic-field gradients.

This apparent anisotropy is not disconcerting because NMR diffusion spectroscopy is exquisitely sensitive to magnetic-field-gradient uniformity, orthogonality, and amplitude. In fact, we propose that the measured diffusion anisotropy in isotropic media can be used to great advantage as the basis for calibrating and aligning magnetic-field gradients. In addition, we suspect that induced eddy currents, nonideal frequency response of the current sources supplying the gradient coils, and slight misalignment (less than 1°) of the gradient directions with respect to the large, steady magnetic field will create a disparity between the b matrix calculated analytically or numerically from the prescribed pulse sequence (using Eq. [6]) and the experimental b matrix (*22*).

As expected, significantly larger differences are observed between diagonal components of the estimated $\mathbf{D}^{\text{eff}}$ for the pork-loin sample than for water, so that water appears isotropic by comparison. Moreover, the ratios of diagonal elements of $\mathbf{D}^{\text{eff}}$ for the pork loin compare very well with those obtained in similar experiments with excised skeletal muscle tissue (*9*).

Errors Introduced by Ignoring Off-Diagonal Components of $\mathbf{D}^{\text{eff}}$ in Spectroscopy and Imaging

Although it is well known that the effective self-diffusion constant varies as an anisotropic sample is rotated with respect to the direction of the applied magnetic-field gradient (*9*), suggesting anisotropic diffusion, only the diagonal elements of the diffusion tensor, D_{xx}, D_{yy}, and D_{zz}, have ever been considered and estimated in these experiments (*8, 9, 15, 27–29*). Since our data suggest that off-diagonal elements may contribute to the measured signal intensity, it is prudent to assess the error in ignoring them in NMR spectroscopy and imaging. A much more detailed analysis is provided in a forthcoming paper (*30*).

Statistically, ignoring the off-diagonal elements in estimating $\mathbf{D}^{\text{eff}}$ is tantamount to performing a constrained multivariate regression in which all off-diagonal elements of $\mathbf{D}^{\text{eff}}$ are set to zero. The F test showed that the off-diagonal elements were very significant in the anisotropic sample, and their significance depended upon the direction of the fibers with respect to the laboratory frame (x, y, and z axes). Physically (or geometrically), setting the off-diagonal elements of $\mathbf{D}^{\text{eff}}$ to zero is equivalent to assuming that the principal (orthotropic) axes of the medium are aligned with the coordinate axes of the laboratory frame of reference, and that the principal diffusivities (eigenvalues of $\mathbf{D}^{\text{eff}}$) equal the diagonal elements of $\mathbf{D}^{\text{eff}}$. Therefore, ignoring the off-diagonal elements in estimating $\mathbf{D}^{\text{eff}}$ precludes the determination of the material's orthotropic axes and, in particular, its fiber orientation (*17*) and may over- or underestimate the true effective diffusivities in the directions parallel and perpendicular to the fiber tracts in anisotropic media (*17*). As an example, consider the rotated pork sample. Using only the largest estimated diffusion coefficient, $D_{xx} = 0.9761 \times 10^{-3}$ mm^2/s, instead of the principal diffusivity, 1.0533×10^{-3} mm^2/s, which is the largest eigenvalue of $\mathbf{D}^{\text{est}}$, results in a percentage error, $\%\Delta E$, in the estimated diffusion distance of the proton, which will depend on the difference of their square roots; i.e.,

$$\%\Delta E = \frac{\sqrt{\lambda_{\max}} - \sqrt{D_{xx}}}{\sqrt{\lambda_{\max}}} = 4\%. \qquad [24]$$

In MR diffusion spectroscopy and imaging, one seldom knows the precise fiber directions of an anisotropic biological or nonbiological specimen a priori.

Potential Applications of the Effective Diffusion Tensor

Once we imbed the estimate of $\mathbf{D}^{\text{eff}}$ in each voxel into an imaging sequence and determine both the principal directions (orthotropic axes) along which diffusive fluxes are uncoupled and the corresponding principal diffusivities in each voxel, we can construct fiber-orientation maps by plotting the fiber tract direction. This procedure is predicated on the assumption that the principal directions of $\mathbf{D}^{\text{eff}}$ coincide with the parallel and perpendicular directions of the fibers (*17*). In addition, the principal diffusivities of $\mathbf{D}^{\text{eff}}$ can be shown to furnish the effective diffusion distances in each of the three principal directions within the anisotropic medium. Consequently, an effective diffusion measurement is made on the scale of a macroscopic voxel to provide estimates of microscopic proton displacements in different directions. Moreover, using the effective diffusion tensor in each voxel, we can construct images of diffusion ellipsoids and scalar invariants of $\mathbf{D}^{\text{eff}}$ which could reveal important microstructural and physiological information about tissues.

Finally, it may be possible to use $\mathbf{D}^{\text{eff}}$ to correct measurement errors caused by misalignment and improper scaling of the time-dependent B field gradients used in diffusion NMR imaging and spectroscopy. Because the effective diffusion tensor is estimated from an equation (e.g., Eq. [10])

in which its coefficients (b matrix elements) scale with $|\mathbf{G}|^2$, $\mathbf{D}^{\text{eff}}$ is inherently more sensitive to the magnetic-field gradient than is the phase, which scales with $|\mathbf{G}|$. This process, formally equivalent to the "whitening" of signals (*31*), can potentially improve the accuracy of pulsed-gradient, spin-echo diffusion NMR spectroscopy and imaging (*17*).

It was suggested recently that diffusion NMR imaging could be performed with species other than water (*32*), such as phosphocholine, phosphocreatine, and *N*-acetylaspartate, all of which have a net charge at physiological pH. Charged moieties may behave differently in response to the applied field gradients, owing to the (Lorentzian) body force they experience. For these media, the diffusion tensor is not necessarily symmetric (*10*). To estimate $\mathbf{D}$ for charged species, we may have to include all six off-diagonal elements instead of only three. Notwithstanding, the estimation methods outlined above should continue to be applicable with this modification.

For this method to be clinically practicable, we must reduce the time required to obtain adequate estimates for each of the effective self-diffusion tensors in each voxel. We do not foresee any obstacles to realizing diffusion *tensor* imaging by obtaining the needed diffusion-weighted images using faster imaging modalities such as echo-planar imaging. Moreover, it may be possible to maximize the information gain per experiment by using improved statistical estimation methods. By this, we mean minimizing the error variances of $\mathbf{D}^{\text{eff}}$ subject to the known constraints. Several independent variables can be manipulated to increase the information gained per experiment, including the total number of trials and the magnetic-field-gradient vector (strength and direction) in each trial. Significant error variance reduction may be achieved by ensuring that the columns of the design matrix are orthogonal (*24*). An optimal experimental protocol may maximize the signal-to-noise ratio for each measurement; it could use a priori information about the coefficients of the diffusion tensor, such as correlations among its components within a voxel and between neighboring voxels. It could also be implemented like a Kalman filter, which uses sampled data to continually update its parameter estimates.

Dependence of Effective Diffusivity on Space and Time

We have explicitly assumed in this paper that diffusion coefficients are independent of space within a voxel. For this condition to be satisfied, we require that the transport of magnetization in the Bloch equation (*19*) be dominated by gradients in the magnetization itself, rather than in the diffusivity; i.e.,

$$\nabla \cdot (\mathbf{D}\nabla\psi) = \frac{\partial}{\partial x_i}\left(D_{ij}\frac{\partial\psi}{\partial x_j}\right) = \frac{\partial D_{ij}}{\partial x_i}\frac{\partial\psi}{\partial x_j} + D_{ij}\left(\frac{\partial^2\psi}{\partial x_j \partial x_i}\right) \approx D_{ij}\left(\frac{\partial^2\psi}{\partial x_j \partial x_i}\right). \quad [25]$$

For this condition to be satisfied, the fractional change in the diffusivity over a voxel must be much less than one, i.e.,

$$\frac{\partial \ln(D_{ij})}{\partial x_i} dx_i \ll 1, \quad [26]$$

where dx_i is the size of the voxel in the x_i direction.

In microscopically heterogeneous systems, the estimated effective self-diffusion coefficients may depend upon the diffusion time. When the approximate diffusion time for a trapezoidal gradient pulse of the experiment is small with respect to the time needed to diffuse to the nearest permeable barrier, $\Delta - \delta/3 \ll \langle r^2 \rangle / D$, the effective diffusion tensor may appear isotropic; when the diffusion time of the experiment is long, the macroscopic molecular displacements will appear more anisotropic. Furthermore, if we monitor a process such as edema, in which the characteristic time of swelling may be significantly longer than the diffusion time of the experiment, the assumption that the diffusion coefficient is independent of time during each experiment may still be valid.

CONCLUSION

We have presented a method for determining the components of $\mathbf{D}^{\text{eff}}$ using robust and efficient linear and nonlinear regression algorithms. Just as the scalar diffusion constant can be estimated by linear regression from spin-echo experiments with isotropic media, we show how the diffusion tensor can be estimated by multivariate regression from spin-echo experiments with anisotropic media. For diffusion in anisotropic media, off-diagonal components of $\mathbf{D}^{\text{eff}}$ vanish only when the "fiber tract" and "laboratory" frames of reference coincide (*17*)—a condition that is rarely verifiable or satisfied in imaging applications. As a result, both diagonal *and* off-diagonal elements of $\mathbf{D}^{\text{eff}}$ must be assumed to affect the measured echo attenuation a priori when $\mathbf{D}^{\text{eff}}$ is estimated. Ignoring the off-diagonal elements of $\mathbf{D}^{\text{eff}}$ is tantamount to discarding the information necessary to determine fiber-tract direction.

ACKNOWLEDGMENTS

This work was performed at the NIH *In Vivo* NMR Center. We thank Alan Olson for his technical support; Robert Turner, Philippe Douek, and Brad Roth for their thoughtful suggestions; Barry Bowman for his editing of the manuscript; and Wolfram Jarisch and Gregory Campbell for useful discussions about optimal experimental design and hypothesis testing, respectively.

REFERENCES

1. H. Y. Carr and E. M. Purcell, *Phys. Ref.* **94**, 630 (1954).
2. E. L. Hahn, *Phys. Rev.* **80**, 580 (1950).

3. E. O. Stejskal and J. E. Tanner, *J. Chem. Phys.* **42,** 288 (1965).
4. D. G. Taylor and M. C. Bushell, *Phys. Med. Biol.* **30,** 345 (1985).
5. K. D. Merboldt, W. Hänicke, and J. Frahm, *J. Magn. Reson.* **64,** 479 (1985).
6. D. LeBihan and E. Breton, *C. R. Acad. Sci. (Paris)* **301,** 1109 (1985).
7. D. LeBihan, *Magn. Reson. Quart.* **7,** 1 (1991).
8. M. E. Moseley, Y. Cohen, J. Kucharczyk, J. Mintorovitch, H. S. Asgari, M. R. Wendland, J. Tsuruda, and D. Norman, *Radiology* **176,** 439 (1990).
9. G. G. Cleveland, D. C. Chang, and C. F. Hazlewood, *Biophys. J.* **16,** 1043 (1976).
10. S. R. DeGroot and P. Mazur, "Non-Equilibrium Thermodynamics," Dover New York, 1984.
11. H. B. G. Casimir, *Rev. Mod. Phys.* **17,** 343 (1945).
12. L. Onsager, *Phys. Rev.* **37,** 405 (1931).
13. L. Onsager, *Phys. Rev.* **38,** 2265 (1931).
14. E. O. Stejskal, *J. Chem. Phys.* **43,** 3597 (1965).
15. R. Turner, D. LeBihan, J. Maier, R. Vavrek, L. K. Hedges, and J. Pekar, *Radiology* **177,** 407 (1990).
16. P. J. Basser, J. Mattiello, and D. LeBihan, Abstracts of the Society of Magnetic Resonance in Medicine, 11th Annual Meeting, Berlin, p. 1222, 1992.
17. P. J. Basser and D. LeBihan, Abstracts of the Society of Magnetic Resonance in Medicine, 11th Annual Meeting, Berlin, p. 1221, 1992.
18. F. Bloch, *Phys. Rev.* **70,** 460 (1946).
19. H. C. Torrey, *Phys. Rev.* **104,** 563 (1956).
20. J. E. Tanner, *J. Chem. Phys.* **69,** 1748 (1978).
21. M. Neeman, J. P. Freyer, and L. O. Sillerud, *J. Magn. Reson.* **90,** 303 (1990).
22. W. S. Price and P. W. Kuchel, *J. Magn. Reson.* **94,** 133 (1991).
23. C. M. Trotter (1980).
24. C. R. Rao, "Linear Statistical Inference and Its Applications," Wiley, New York, 1965.
25. P. R. Bevington, "Data Reduction and Error Analysis for the Physical Sciences," McGraw–Hill, New York, 1969.
26. G. W. Snedecor and W. G. Cochran, "Statistical Methods," 8th ed., Iowa State Univ. Press, Ames, 1989.
27. T. L. Chenevert, J. A. Brunberg, and J. G. Pipe, *Radiology* **177,** 401 (1990).
28. P. Douek, R. Turner, J. Pekar, N. Patronas, and D. LeBihan, *J. Comput. Assist. Tomogr.* **15,** 923 (1991).
29. G. D. Fullerton, I. L. Cameron, and V. A. Ord, *Radiology* **155,** 433 (1985).
30. J. Mattiello, P. J. Basser, and D. LeBihan, *J. Magn. Reson.*, in press.
31. K. Fukunaga, "Introduction to Statistical Pattern Recognition," Academic Press, New York, 1972.
32. D. LeBihan, C. A. Cuenod, and S. Posse, Abstracts of the Society of Magnetic Resonance in Medicine, 11th Annual Meeting, Berlin, p. 1218, 1992.